Bioconjugate Chemistry

Article

pubs.acs.org/bc

PNA-Induced Assembly of Fluorescent Proteins Using DNA as a Framework

Zahra Gholami,[†] Luc Brunsveld,[‡] and Quentin Hanley*,[†]

[†]School of Science and Technology, Nottingham Trent University, Clifton Lane, Nottingham NG11 8NS, United Kingdom

[‡]Eindhoven University of Technology, Department of Biomedical Engineering, Laboratory of Chemical Biology, PO Box 513, 5600 MB, Eindhoven, The Netherlands

ABSTRACT: Controlled alignment of proteins on molecular frameworks requires the development of facile and orthogonal chemical approaches and molecular scaffolds. In this work, protein−PNA conjugates are brought forward as new chemical components allowing efficient assembly and alignment on DNA scaffolds. Site-selective monomeric teal fluorescent protein (mTFP)−peptide nucleic acid (PNA) (mTFP-PNA) conjugation was achieved by covalent linkage of the PNA to the protein through expressed protein ligation (EPL). A DNA beacon, with 6-Fam and Dabcyl at its ends, acts as a framework to create an assembled hetero-FRET system with the mTFP-PNA conjugate. Using fluorescence intensity, frequency domain lifetime measurements, and anisotropy measurements, the system was shown to produce FRET as indicated by decreased donor intensity, decreased donor lifetime, and increased donor anisotropy. Extension of the DNA scaffold allowed for the assembly of multiple mTFP-PNA constructs. Efficient formation of protein dimers and oligomers on the DNA-PNA frameworks could be shown, as visualized via size exclusion chromatography (SEC) and electrophoresis (SDS-PAGE). Assembly of multiple proteins in a row induced homo-FRET for the mTFP-PNA's assembled on the DNA scaffolds. The oligonucleotide framework allows an induced and controllable assembly of proteins by fusing them to PNAs directed to align on DNA scaffolds.

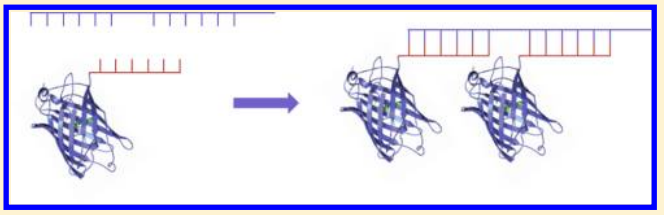

INTRODUCTION

Controlled assembly is of great importance in the modulation, localization, and interactions of proteins. For example, assembly of proteins plays an important role in vital biological process such as signal transduction,[1−3] transcription,[4] and formation of fibers and filaments.[5−7] Well-defined synthetic protein assemblies allow for molecular insights and targeting of biological processes.[8−17] Nevertheless, the molecular characteristics and diversity of protein chemistry makes designing accurate and specific self-assembled systems based on proteins a challenging endeavor. DNA possesses unique recognition capabilities as a scaffold to address precise and programmed self-assembled nanostructures.[18,19] The combination of the unique programmability of DNA-directed self-assembly and the versatility of functional proteins can be provided by semisynthetic DNA−protein conjugation techniques. DNA−protein conjugates have been used as controllable templates to mimic self-assembled protein complexes in biological systems.[19−21] For example, DNA−protein conjugates were applied in assembly of enzymatic networks,[22,23] highly ordered protein arrays,[16,24] and biomolecular delivery systems.[25]

Despite the wide development of DNA-directed assembly systems, the high negative charge density of DNA may limit its practical application as a scaffold in self-assembled protein systems. Peptide nucleic acid (PNA) is a DNA mimic in which the regular phosphodiester backbone has been replaced by a pseudopeptide skeleton.[26,27] PNA binds to the complementary DNA and RNA through Watson−Crick base pairs with high affinity and sequence specificity.[28] PNA provides better stability than DNA duplexes, even for short sequences, and has higher mismatch sensitivity.[26,27] Moreover, unlike the DNA backbone, the pseudopeptide skeleton can be altered by replacing glycine with different amino acides, such as lysine or cysteine, to provide reactive amine or thiol groups to conjugate the PNA to proteins.[27] Expressed protein ligation (EPL) is a semisynthetic version of native chemical ligation enabling the site-selective attachment of synthetic constructs to proteins.[29] EPL has been used previously for the construction of a variety of peptide−protein[30,31] and protein−PNA conjugates.[32] EPL typically makes use of a recombinant protein containing a thioester or cysteine at the C- or N-terminus.[33−35] A protein with a C-terminal thioester provides a conjugation site for a PNA with an N-terminal cysteine, enabling a ligation via a native peptide bond.[36,37] Applying EPL to fluorescent proteins (FP) to create FP-PNA conjugates (Scheme 1) provides an ideal system for studying controlled protein assembly: (i) it provides precise control over the exact composition and structure of an inducibly assembled system following addition of a DNA template; (ii) it allows fundamental insights into the behavior of proteins in self-assembled architectures to be gained by observing the photophysical behavior of assembled FPs. Two relevant photophysical strategies that can be employed to

Received: April 19, 2013
Revised: June 24, 2013
Published: July 14, 2013

   dx.doi.org/10.1021/bc400202s | *Bioconjugate Chem.* 2013, 24, 1378−1386

Scheme 1. mTFP-PNA Ligation Using Native Chemical Ligation (NCL)[a]

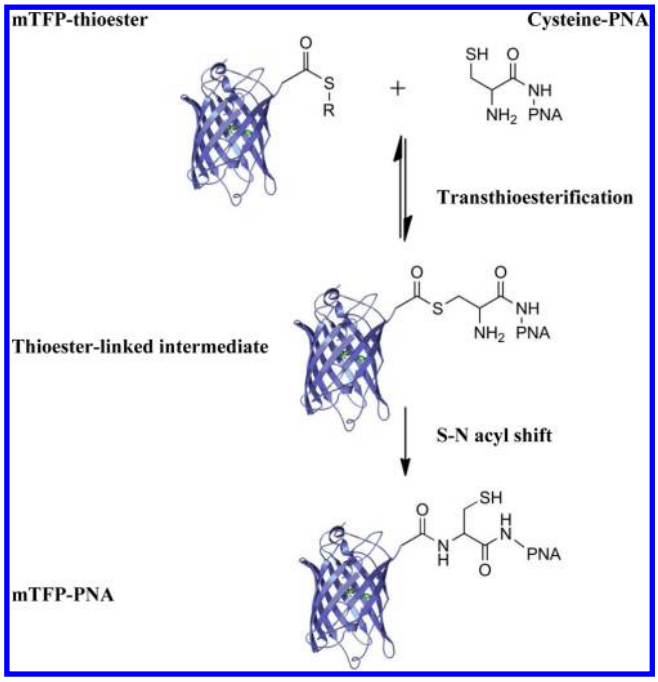

[a]NCL is based on the transthioesterification reaction of mTFP-thioesters with thiol groups of PNA N-terminal cysteine. Transthioesterification with the thiol group of N-terminal cysteine generates a thioester-linked intermediate which spontaneously undergoes a rapid intramolecular S−N transfer forming a native peptide bond between mTFP and PNA.

observe template directed assembly of FP-PNA monomer units are: (i) assembly along a complementary DNA and detection via Förster resonance energy transfer (FRET) among like fluorophores (homo-FRET) (Scheme 2); and (ii) assembly with a DNA beacon and detection via conventional FRET (hetero-FRET) (Scheme 3). DNA beacons have been widely used for sequence recognition in biology, chemistry, medical sciences, and biotechnology since they were reported in 1996.[38] A variety of such beacons based on chimeric DNA-PNA and purely PNA beacons have been reported to provide stronger binding to templates.[39,40]

Scheme 3. DNA Beacon Structure in Closed and Open forms[a]

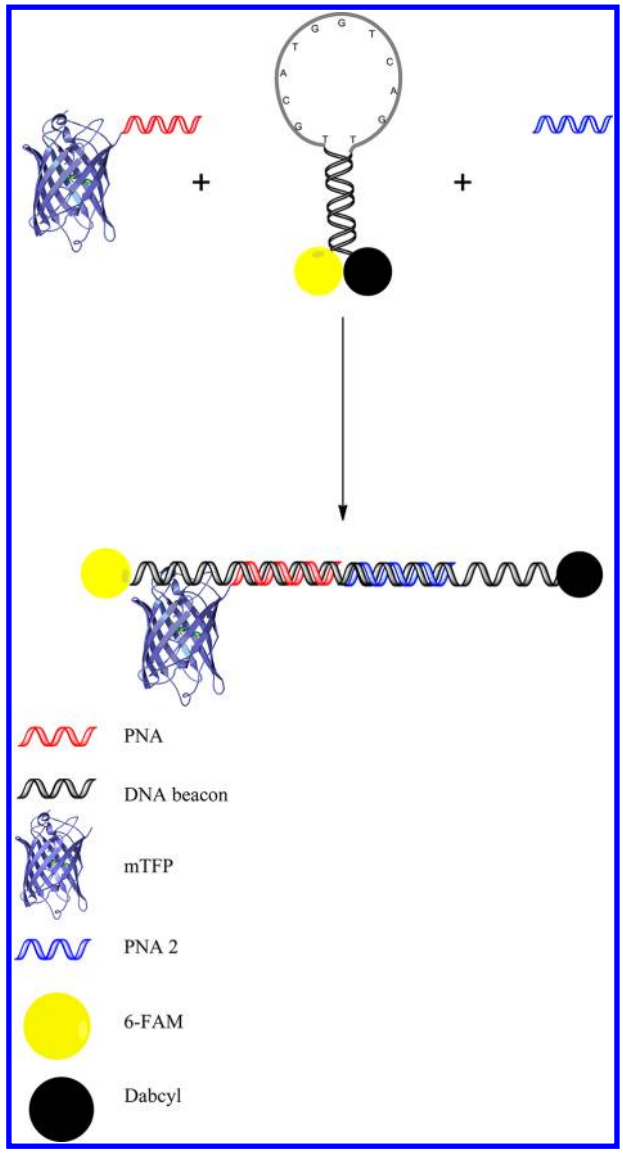

[a]In the assembled system hetero-FRET can occur to both the 6-FAM and the Dabcyl group.

Scheme 2. Assembly of mTFP in Tetramer Form Using DNA2 as a Framework

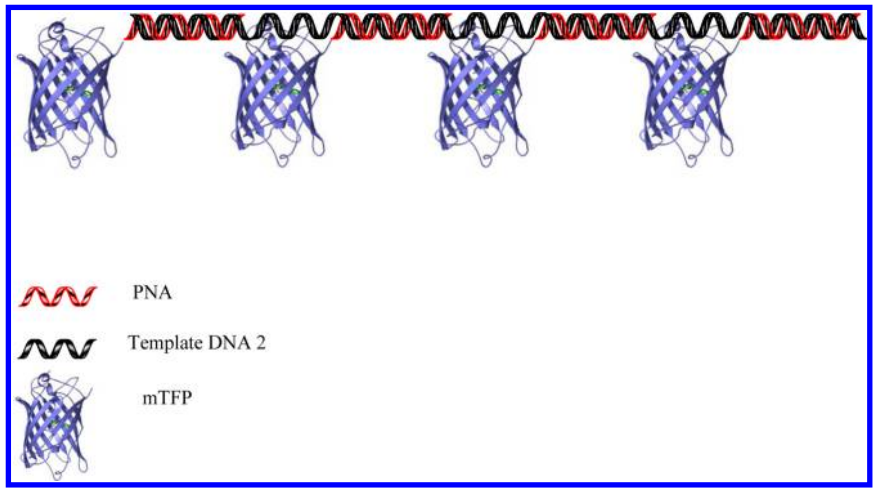

dx.doi.org/10.1021/bc400202s | Bioconjugate Chem. 2013, 24, 1378−1386

This study reports a programmable model system allowing precise control over the assembly of proteins directed by the molecular recognition capabilities of PNA-DNA architectures. EPL allowed the creation of well-defined FP-PNA monomer units (Scheme 1). Subsequent assembly was directed by engineered DNA templates (Schemes 2 and 3). Unlabeled DNA templates enabled assembly of FPs into protein dimer and tetramer homo-FRET systems, which were studied using fluorescence anisotropy. A complementary DNA beacon hetero-FRET system, enabling single binding detection, was studied with fluorescence intensity and lifetime measurements. The photophysical methods, combined with mass spectrometry, SDS-PAGE, and size exclusion chromatography experiments, highlight the inducible formation of supramolecular protein assemblies on a predetermined scale.

EXPERIMENTAL PROCEDURES

Reagents. All reagents, including sodium 2-mercaptoethansulfonate (MESNA), 4-mercaptophenylacetic acid (MPAA), and *tris*(2-carboxyethyl phosphine (TCEP), were purchased from Sigma-Aldrich unless specifically noted.

Protein Expression and Purification. Monomeric teal fluorescent protein (mTFP) with an N-terminal 6-His-tag was expressed in *E. coli* using plasmid pHT581 possessing a C-terminal engineered intein and chitin binding domain (CBD), analogues to previously described compounds.[41] A thioester group was introduced at the C-terminus of the protein through cleavage of the intein using MESNA, and the resulting protein was purified using chitin binding affinity chromatography. Chitin resin (New England Biolabs) was transferred to a 10 mL disposable chromatography column (Biorad) and equilibrated with 10 volumes of washing buffer (Na_2HPO_4 (19.3 mM), NaH_2PO_4 (25 mM), NaCl (500 mM), EDTA (0.5 mM) in distilled deionized water. Cleavage of the intein-tag fused to the C-terminus of mTFP was performed through incubation of loaded proteins with 20 mL elution buffer (Na_2HPO_4 (23.2 mM), NaH_2PO_4 (25 mM), NaCl (100 mM), EDTA (0.5 mM), MESNA (400 mM) in ddH_2O, pH 7.5) in the dark with slow shaking overnight at room temperature. Afterward, the cleavage buffer was replaced by storage buffer (Na_2HPO_4 (19.3 mM), NaH_2PO_4 (25 mM), NaCl (50 mM), EDTA (0.1 mM), in ddH_2O (pH 7). The collected proteins were concentrated by centrifugation at 3700 *g* using centrifugal filter tubes (Amicon 10000 MW, Millipore) for 10−16 min several times to remove the MESNA. The resulting mTFP was further purified using His-tag affinity chromatography. To prepare the Ni-NTA resin, it was washed with 2−3 column volumes of distilled water. Nickel sulfate solution (50 mM) was added to the column followed by washing with distilled water and His-tag buffer (Na_2HPO_4 (19.3 mM), NaH_2PO_4 (25 mM), NaCl (50 mM), EDTA (0.1 mM) in ddH_2O, imidazole (20 mM), pH 7). After loading of the protein, the column was washed again with 10 mL of His-tag washing buffer and the proteins eluted using 4 mL His-tag elution buffer (Na_2HPO_4 (19.3 mM), NaH_2PO_4 (25 mM), NaCl (50 mM), EDTA (0.1 mM) in ddH_2O, imidazole (250 mM), pH 7). The final concentration of purified proteins was determined by UV−visible spectrophotometer at 280 nm (Perkin-Elmer, Lambda 25 UV/vis spectrometer). The final yield of mTFP-thioester was about 8 mg/mL, purity was confirmed with SDS-PAGE, and the protein was stored at −80 °C.

mTFP-PNA Ligation. Reactions were run on a 100 μL scale using 4-fold excess of PNA. The ligation solution was 100 μM mTFP in storage buffer (Na_2HPO_4 (19.3 mM), NaH_2PO_4 (25 mM), NaCl (50 mM), EDTA 0.1 mM, in ddH_2O pH 7), 400 μM PNA1 (ACGTAC) (Advanced peptide Inc., USA), 70 mM TCEP (in H_2O, pH 7) as a reducing agent, and 50 mM MPAA as a catalyst. The solutions were incubated at room temperature for 60 min. These conditions were selected after evaluating the effects of MPAA (0−200 mM), PNA (400, 600, and 700 μM), and incubation time (20−485 min and overnight) on the ligation reaction while maintaining other conditions constant.

The product was isolated using centrifugal filter tubes (Amicon 10000 MW, Millipore) at 13 000 rpm. The retained portion was resuspended in 70 mM TCEP, incubated, and centrifuged several times to reduce disulfide bond generated at the ligation site. The mTFP-PNA conjugate was subsequently stored at 4 °C (short times) or −20 °C (long-term storage). Products were analyzed by MALDI-TOF MS and yields quantified by UV−vis spectrophotometry. Ligation samples were diluted and their absorbance at 260 nm measured to estimate PNA concentration. The extinction coefficient of PNA was estimated based on the published values for the molar extinction coefficients of PNA bases.[37] Pure mTFP absorbance at 260 nm was measured and subtracted from the mTFP-PNA absorbance.

Hybridization and Assembly of mTFP-PNA with DNA. Hybridization of mTFP-PNA to DNA beacon (6FAM5′ACAGCTGCATGGTCAGTGCTGT3′Dabcyl) (The Midland Certified Reagent Company, Inc., USA) was assessed by SEC-HPLC (SRT SEC-150, 5 μm, 4.6 × 300 mm; Chromex Scientific, UK) calibrated with molecular weight protein marker kit 12−200 kDa (Sigma). Varying concentrations of a DNA Beacon: PNA2 (CAGTCA) (Advanced peptide Inc., USA) (0−27 μM) were incubated with 2.5 μM purified mTFP-PNA solution.

Two DNA sequences (DNA1 5′TGCATGGATCTGCATG3′and DNA2: 5′TGCATGGATCTGCATGGATCTGCATGGATCTGCATG3′) (Life technologies corporation, USA) were used to make assembled mTFP-PNA dimers and tetramers, respectively (Note: The PNA:DNA mediated protein assemblies are referred to by the number of proteins assembled; e.g., a dimer consists of two proteins and the DNA scaffold and a tetramer of four proteins and the DNA scaffold). The hybridization of DNA to mTFP-PNA was determined by SDS-PAGE electrophoresis. 1.25 μM DNA1 and 0.62 μM DNA2 were titrated with different concentrations of mTFP-PNA (1.25−2.5 μM and 0.62−2.5 μM for dimer and tetramer assembly, respectively) in phosphate buffer (100 mM, NaCl (200 mM), pH 7) with 2 h incubation at room temperature. The results were assessed by SEC-HPLC at 214 and 462 nm using phosphate buffer (150 mM, pH 7) as mobile phase.

Photophysical Measurements. Different concentrations of DNA1 and DNA2 (0−2.5 μM) were added to 2.5 μM mTFP-PNA and the emission intensity and anisotropy recorded between 480 and 530 nm using a fluorimeter equipped with polarizers (Cary Eclipse; Varian). Fluorescence lifetimes were measured using a spectroscopic fluorescence lifetime imaging system operating in the frequency domain[42] with rhodamine 6G as a lifetime reference. Energy transfer efficiency (E) can be estimated based on R_0 (the Förster distance in which the transfer efficiency E is 50%) and r (distance between fluorophores) (eq 1).[43]

$$E = \frac{R_0^6}{R_0^6 + r^6} \tag{1}$$

In the case of heterotransfer this can be assessed by lifetimes or intensity

$$E = 1 - \frac{\tau_2}{\tau_1} \qquad E = 1 - \frac{I_2}{I_1} \tag{2}$$

where τ_1 and I_1 are the lifetime and intensity of the donor in the absence of acceptor, and τ_2 and I_2 are the lifetime and intensity in the presence of the acceptor.

When frequency domain lifetime measurements are used, the measured phase, ϕ_i, and modulation, m_i, may be presented in polar coordinates.

$$x_i = m_i \cos(\phi_i) \tag{3}$$

$$y_i = m_i \sin(\phi_i) \tag{4}$$

In polar coordinate analysis, the fraction of mTFP-PNA in the hybridized form (α) can be calculated based on the following equation:

$$\alpha = \sqrt{\frac{(x_1 - x_i)^2 + (y_1 - y_i)^2}{(x_1 - x_2)^2 + (y_1 - y_2)^2}} \tag{5}$$

where (x_1, y_1), (x_2, y_2), and (x_i, y_i) are the coordinates in the absence of acceptor, the fully hybridized form, and mixture of free and hybridized forms, respectively.

Lifetime does not change in the case of homotransfer. As a result the fluorescence anisotropy is a useful indicator of assembly. To a first approximation, the anisotropy of an oligomer of fluorophores undergoing homo-FRET, r_{oligomer}, is the anisotropy in a monomer, r_{monomer}, divided by the number of fluorophores, n, in the oligomer.

$$r_{\text{oligomer}} \cong \frac{r_{\text{monomer}}}{n} \tag{6}$$

This approximation only applies when the interfluorophore distance is <0.8 R_0. In more complex cases, treatment of homo-FRET is more difficult, depending on the cluster size, the orientation between fluorophores, and interfluorophore distances.[44,45]

Competing with homo-FRET depolarization are the opposing effects of greater molecular weight. This phenomenon can be understood through the Perrin equation:[43]

$$r = \frac{r_0}{1 + \frac{\tau}{\theta}} \tag{7}$$

where τ is the fluorescence lifetime, θ is the rotational correlation time, and r and r_0 are measured and initial anisotropy, respectively. The rotational correlation time depends on viscosity, η, the molecular weight, M, the specific volume and hydration, $\bar{\nu} + h$, the gas constant, R, and the temperature, T.

$$\theta = \frac{\eta M}{RT}(\bar{\nu} + h) \tag{8}$$

Assuming all other parameters are equal (temperature, viscosity, etc.), the rotational correlation time scales with the mass indicating that as mass increases, the measured r will approach r_0.

$$\frac{\theta_1}{\theta_2} \cong \frac{M_1}{M_2} \tag{9}$$

RESULTS AND DISCUSSION

Synthesis and Characterization mTFP-PNA. *Ligation and Purification of mTFP-PNA.* The monomeric TFP (mTFP) was chosen for its greater brightness and photostability when compared to CFP variants and its ability to form good FRET pairs with the YFP variants, mKate, mKO2, and tdTomato.[46−50] The mTFP was expressed with a thioester group at the C-terminus by the intein based method and purified using chitin and His-tag affinity chromatography. Mass spectrometry identified the integrity of the protein (measured m/z 27 969 ± 6 Da, calculated m/z 27 965 Da) and SDS-PAGE (28 kDa) showed the purity of the resulting mTFP-thioester.

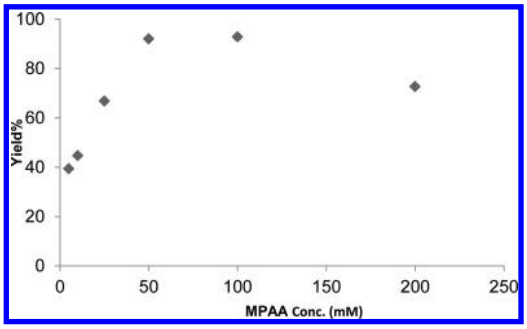

Figure 1. Ligation yield (%) vs MPAA (5−200 mM) with a 60 min reaction time at room temperature measured by UV spectrophotometry.

Kinetic Studies of Ligation to Form mTFP-PNA. The reaction of 100 μM purified mTFP-thioester group with excess (400 μM) cysteine-PNA1 was studied in the presence and absence of 50 mM MPAA catalyst at pH 7 and variable incubation times (20 min to 18 h) at room temperature. Mass spectrometry results showed that the MPAA catalyst was required for the ligation of PNA to mTFP to proceed. The hydrolyzed mTFP exhibited a peak at m/z 27 833 ± 7 Da (calculated m/z 27 844 Da) and the mTFP-PNA product at m/z 29 560 ± 6 Da (calculated m/z 29 555 Da). An additional peak at m/z 31 293 ± 7 Da (calculated m/z 31 286 Da) indicated partial double PNA attachment to mTFP. Incubation with the reducing agent TCEP followed by centrifugation assisted dialysis efficiently removed the second attached PNA; since native mTFP does not feature a cysteine, the second PNA was most probably attached via disulfide bond formation to the newly introduced SH group at the ligation site. HPLC analysis of the final product confirmed purity and integrity of the mTFP-PNA with a yield near 100%.

Effect of Catalyst and PNA Concentration on mTFP-PNA Ligation Yield. To elucidate the effect of catalyst concentration on mTFP-PNA ligation, varying concentrations of MPAA (5−200 mM) were added to the ligation reaction of the PNA to the fluorescent protein. All components were mixed at pH 7 and incubated for 60 min. The conversion was studied by spectrophotometry using the estimated absorbance of the mTFP-PNA at 260 nm as an indicator of the ligated PNA concentration and it was compared with the calculated absorbance of 100% ligation of PNA to mTFP (1:1 ratio) to obtain the final percent yield. The results confirmed >90% yield. The yield increased monotonically with added catalyst up

dx.doi.org/10.1021/bc400202s | Bioconjugate Chem. 2013, 24, 1378−1386

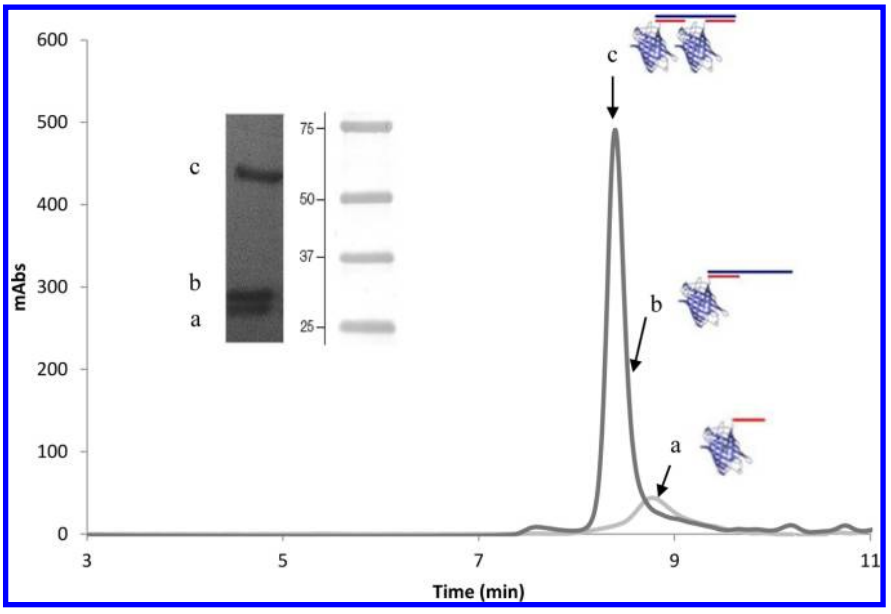

Figure 2. SEC-HPLC chromatograms of mTFP-PNA (gray line, peak at 8.7 min) and mTFP-PNA-DNA1 (black line, peak at 8.3 min related to DNA1:dimer). Inset: SDS−PAGE bands at 29, 33, and 63 kDa, respectively, related to: (a) monomer, (b) DNA1:monomer, (c) DNA1:dimer (left), standard protein ladder (right).

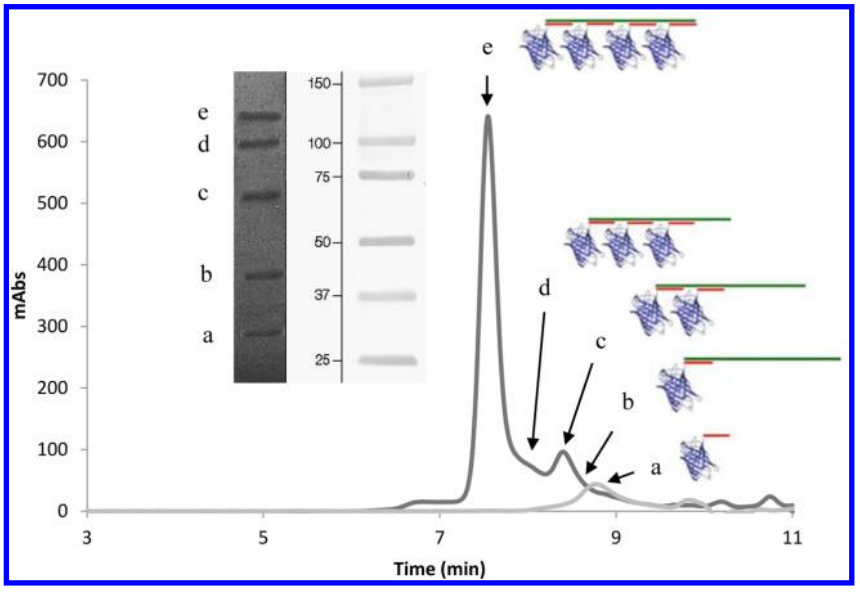

Figure 3. SEC-HPLC chromatograms of mTFP-PNA (gray line, peak at 8.7 min) and mTFP-PNA-DNA2 (black line, peak at 7.5 and 8.3 min related to tetramer:DNA2 and dimer:DNA2, respectively). Inset: SDS-PAGE results show bands at 29, 40, 70, 99, and 129 kDa, respectively, related to: (a) monomer, (b) monomer:DNA2, (c) dimer:DNA2, (d) trimer:DNA2 and tetramer:DNA2 (left), standard protein ladder (right).

to 100 mM (Figure 1). Based on the data, 50 mM catalyst was selected for subsequent ligation experiments. The PNA:mTFP ratio was optimized by adding different concentrations of PNA (400−600 and 700 μM) to the ligation solution. The spectrometry data showed that a high ratio of PNA:mTFP resulted in more evidence of a second attached PNA at 60 min ligation time. Therefore, an optimized ratio of 4:1 was used in all ligation experiments.

Size Exclusion Analysis of mTFP-PNA:DNA Assemblies. *Assembly of mTFP-PNA in Dimer and Oligomer Forms.* In order to test whether the model system could assemble FPs, DNA sequences containing either two (DNA1) or four (DNA2) complementary parts, each of which could hybridize to an mTFP-PNA, were selected as frameworks for directed assembly (Scheme 2). SDS−PAGE analysis of a 2:1 ratio of mTFP-PNA:DNA1 showed three distinct bands at 29, 33, and 63 kDa related to mTFP-PNA monomer, monomer:DNA1, and dimer: DNA1 (Figure 2 inset). Similarly, oligomer assembly with a 4:1 of ratio of mTFP-PNA:DNA2 indicated five distinct bands at 29, 40, 70, 99, and 129 kD attributed to mTFP-PNA monomer, monomer:DNA2, dimer:DNA2, trimer:DNA2, and tetramer:DNA2 (Figure 3, inset).

The SEC-HPLC was calibrated with molecular weight standard and the chromatogram of mTFP-PNA showed a single peak (8.7 min) when monitored at 462 nm (maximum absorption of mTFP) and 214 nm (general absorption of all components), in line with the expected molecular mass of a monomeric construct. A solution featuring a 2:1 ratio of mTFP-

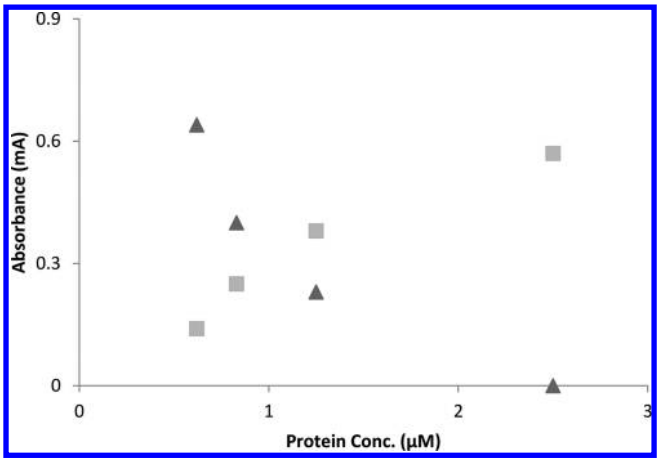

Figure 4. SEC analysis of showing the increase of the tetramer peak (7.5 min ■) and decrease of the monomer peak (8.7 min ▲) monitored at 462 nm while titrating DNA2 (0.62 μM) with mTFP-PNA (0.62–2.5 μM).

PNA:DNA1 showed a new single peak at 8.3 min, indicating the efficient formation of a protein dimer assembled on the DNA scaffold (Figure 2). A mixture of the mTFP with the longer DNA scaffold DNA2 with a 4:1 ratio of mTFP-PNA:DNA2 resulted in additional peaks (Figure 3). The highest related to the formation of an assembled protein tetramer. A titration of DNA2 with increasing amounts of mTFP-PNA showed a gradual decrease of the peak corresponding to the mTFP-PNA monomer (8.7 min) (Figure 4). The monomer peak reached zero at a 4:1 ratio of mTFP-PNA to DNA2. Simultaneously, a concomitant increase in assembled protein tetramer was observed (7.5 min). The complete disappearance of the monomeric form of mTFP-PNA in the chromatogram upon addition of DNA shows that protein assembly formation is very effective. After addition of excess DNA2, unbound DNA2 could also be observed in the chromatogram (12 min).

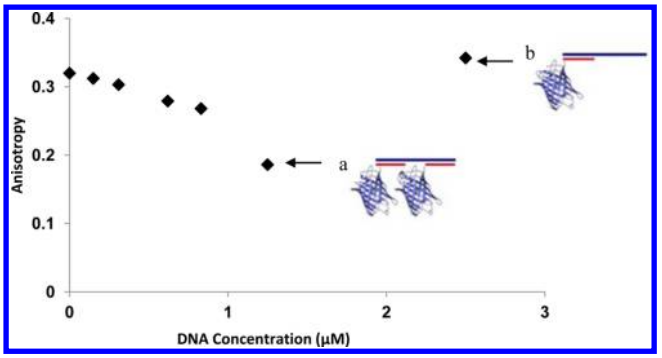

Figure 6. Anisotropy changes of the DNA1-mTFP-PNA system after adding different concentration of DNA1 (0–2.5 μM) to 2.5 μM mTFP-PNA (a) 1.25 μM: DNA1-dimer and (b) 2.5 μM: DNA1-monomer. The anisotropy decreases due to homo-FRET induced depolarization until the equivalence point (2 mTFP-PNAs to 1 DNA1) is reached (a). After equivalence is reached, anisotropy increases due to the formation of 1:1 complexes (mTFP-PNA:DNA1). Note that the anisotropy at the point (b) is slightly greater than before addition of any DNA due to the increased rotational correlation time (eq 8) of the 1:1 (mTFP-PNA:DNA1) complex relative to free mTFP-PNA.

Photophysical Studies of mTFP-PNA:DNA Assemblies. *FRET Occurrence after Hybridization of mTFP-PNA to DNA Beacon.* To demonstrate a hetero-FRET system, a DNA beacon (6FAM5′ACAGCTGCATGGTCAGTGCTGT3′ Dabcyl) (6-Fam: λ_{ex}: 494 nm and λ_{em}: 521 nm) was designed to create a FRET pair with one mTFP-PNA (mTFP: λ_{ex}: 462 nm and λ_{em}: 492 nm). No fluorescence was observed from the closed form of the DNA beacon, because of Fam quenching by the Dabcyl group. In the presence of mTFP-PNA or PNA2 (CAGTCA), which are each complementary to the DNA beacon loop sequence (5′-TGCATGGTCAGT-3′), the conformation of the DNA beacon changed to the open form and emission at 521 nm appeared (Scheme 3). Three phenomena indicative of FRET were observed, including: (1) quenched

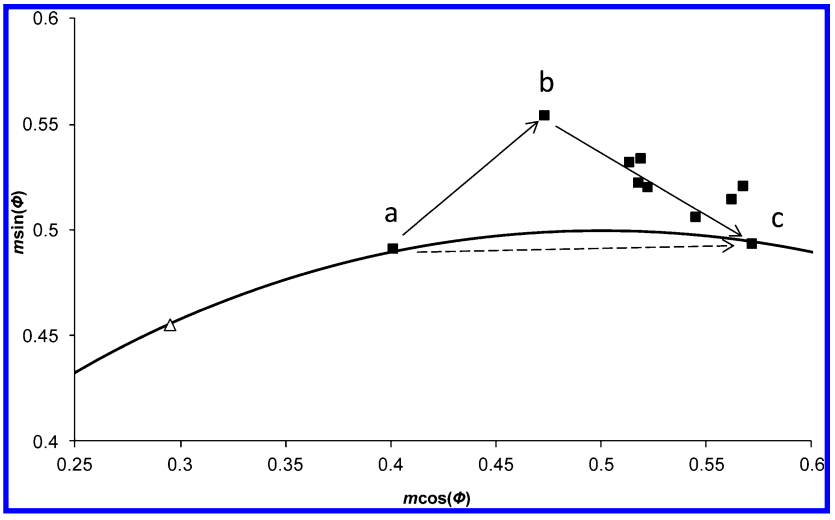

Figure 5. Polar coordinate presentation of frequency domain lifetime measurements from mTFP-PNA:Beacon:PNA2 complexes. The data correspond to measurements dominated by 6-FAM (■). The position of the rhodamine 6G standard is also shown (△). Position (a) indicates the position of mTFP-PNA in the absence of added Beacon:PNA2 and corresponds 3.3 ns. Position (b) represents the position of a mixture of mTFP-PNA (2.5 μM) and Beacon:PNA2 (2.7 μM). As the concentration of Beacon:PNA2 increases relative to mTFP-PNA the system follows the trajectory from (b) to (c). At point (c) the signal is dominated by Beacon:PNA2 (2.4 ns). The dotted arrow represents the expected path of a noninteracting mixture of mTFP-PNA and Beacon:PNA2.

dx.doi.org/10.1021/bc400202s | *Bioconjugate Chem.* 2013, 24, 1378–1386

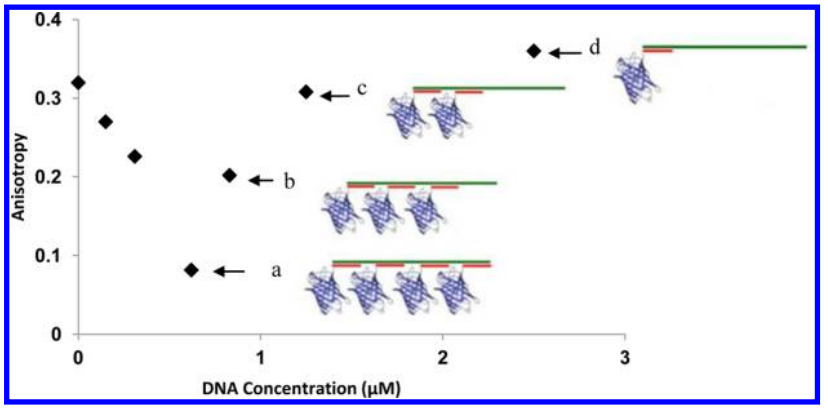

Figure 7. Anisotropy changes of the DNA2-mTFP-PNA system after adding different concentration of DNA2 (0−2.5 μM) to 2.5 μM mTFP-PNA (a) 0.62 μM:DNA2-tetramer, (b) 0.83 μM:DNa2-trimer, (c) 1.25 μM:DNA2-dimer, and (d) 2.5 μM:DNA2-monomer). The assemblies illustrated at points a, b, and c represent the stoichiometry. The mixtures of assembled species at these locations are more complex. For example, the 2:1 species can exist in 3 forms and a randomly assembled system will include some amount of 1:1, 2:1, 3:1, and 4:1 species. As with the dimer system (Figure 6) the trend in anisotropy follows the extent of homo-FRET which tracks the extent of assembly. Homo-FRET is maximal (minimum anisotropy) at the equivalence point (4:1 mTFP-PNA to DNA2). Addition of further template after equivalence is reached causes the anisotropy to increase until all mTFP-PNAs are in 1:1 complexes. Note that the 1:1 complex of mTFP-PNA to DNA2 has a higher anisotropy (d) than free mTFP-PNA.

donor emission; (2) frequency domain lifetimes in the acceptor region exhibiting τ_ϕ greater than τ_m; and (3) increased donor anisotropy.

Intensity Measurements. Varying concentrations of DNA beacon:PNA2 (0−27 μM) were combined with 2.5 μM of the mTFP-PNA solution. An increase of the DNA beacon correlated with a decrease of donor (mTFP-PNA) emission, due to energy transfer to 6-FAM on the beacon. The mTFP-PNA:Beacon:PNA2 assembly (2.5 μM mTFP-PNA:27 μM DNA; beacon at saturating conditions) exhibited a 59 ± 4% energy transfer over the range of 490−510 nm relative to a control sample of mTFP:DNA beacon. Control samples consisting of mTFP:DNA beacon resulted in up to 40% intensity decrease when added to unligated mTFP, which can be ascribed to inner filter effects[37] arising from the highly colored solution seen with the highest beacon concentrations and slight quenching effect of Dabcyl when the fluophores are in 7 nm distance in open form (R_0: 4.6 nm[51]). Similar effects were not observed with dilute solutions (e.g., 2.7 μM DNA beacon). To correct for this, energy transfer efficiencies (eq 2) were computed relative to the control solutions of mTFP:beacon.

Lifetime Measurements. The mTFP-PNA:Beacon:PNA2 system exhibited changes in frequency domain lifetime characteristics upon assembly (Figure 5). In the absence of DNA Beacon, mTFP-PNA exhibited a single component lifetime of 3.3 ns. Under conditions of high excess Beacon:PNA2, the system was dominated by free Beacon:PNA2 (2.4 ns). At near stoichiometric conditions, the acceptor 6-FAM exhibited lifetime heterogeneity with τ_ϕ (3.1 ns) greater than τ_m (2.5 ns). This behavior is characteristic of FRET and results in the appearances of points outside the semicircle of single component lifetimes in a polar plot (Figure 5).[52,53] These data are consistent with partial unfolding of the Beacon in the presence of PNA2 and with the production of an assembled system of mTFP-PNA:Beacon:PNA2 in which there is energy transfer from mTFP to 6-FAM.

Assembly of mTFP-PNA with DNA Beacon. In this hetero-FRET system, the modification and assembly of mTFP were accompanied by a small increase in mTFP fluorescence anisotropy. The anisotropy of mTFP was initially 0.32 and increased after PNA1 ligation to 0.33. Subsequent hybridization of mTFP-PNA1 to the DNA beacon yielded a further increase in r to 0.35. The calculated correlation times (eq 7) for mTFP-PNA1 (θ_1) and mTFP-PNA1:DNA (27 μM DNA) (θ_2) were 18 and 25 ns, respectively, using experimentally determined average lifetimes and r_0 = 0.39 from previous studies of fluorescent proteins.[54] These estimated rotational correlation times are in the typical range of monomeric fluorescent FPs in buffer.[36] The observed 27% increase in θ when mTFP-PNA1 (29 560 Da) formed the mTFP-PNA1:Beacon assembly (33 241 Da) was consistent with the 12% increase in mass. These results were interpreted as reinforcing the intensity and polar plot analyses which together proved the ligation and assembly strategy was successful and the assemblies accessible to photophysical analysis.

Anisotropy Measurements of Homo-FRET System Demonstrating Dimer and Oligomer Assembly. Anisotropy changes of the system were studied by adding a range of DNA1 and DNA2 concentrations (0−2.5 μM) to 2.5 μM of mTFP-PNA. Maximal anisotropy values of 0.34 (DNA1) and 0.36 (DNA2) were observed when the ratio of mTFP-PNA to DNA1 and DNA2 (monomer) was at 1:1. These were slightly higher than observed for free mTFP-PNA (0.32) and consistent with a slight increase in the rotational correlation time in the larger assemblies and similar to values measured in the presence of DNA beacon. A homo-FRET system was prepared by adding mTFP-PNA to a complementary DNA template (DNA1 or DNA2) which produced a decrease in measured anisotropy. Titration of mTFP-PNA with DNA1 resulted in a gradual decrease of anisotropy compared to mTFP-PNA:DNA1 monomer (Figure 6). The maximum decrease of 45% was observed in the presence of 2:1 ratio of mTFP-PNA to DNA1, close to the predicted 50% (eq 6). Thereafter, the anisotropy gradually increased on addition of more mTFP-PNA (Figure 6).

In template directed oligomer formation via DNA2, a 15% decrease in anisotropy was obtained with a 2:1 ratio of mTFP-PNA:DNA2. This value is significantly different than predicted by eq 6. However, DNA2 has 4 locations to bind, and with two mTFPs attached, the distance between monomer units is expected to range from 3.3 to 10 nm. The larger distances are

outside 0.8 R_0[44,55] resulting in less change in anisotropy than seen in the DNA1 assembly. Similarly, when the ratio of mTFP-PNA to DNA2 was 3:1 a 44% decrease was observed. The lowest anisotropy (0.082) was obtained with a 4:1 ratio. The resulting template directed tetramer assembly was in reasonable agreement with the predictions of eq 6 (Figure 7).

■ CONCLUSION

In summary, the self-assembled fluorescent protein model system based on PNA conjugates demonstrates a new way to take control of protein assembly. The unique structure and characteristics of PNA and the capability of studying the current model system with fluorescence measurements make it a promising system to study protein assemblies under controlled conditions. This study demonstrates that PNA can efficiently conjugate to proteins with high specificity via expressed protein ligation. Taking advantage of the precise recognition characteristics of PNA for complementary oligonucleotides, directed assembly proceeded conveniently to the formation of dimers and higher oligomers. The assemblies gave clear and readily interpreted photophysical signatures creating a practical tool to study the behavior of protein aggregates. By fusing EPL enabled FPs to targets of interest, such as receptors, control of both assembly and visualization is provided following addition of template to PNA ligated proteins. This approach could be extended to study aggregation behavior in both biochemical and cellular environments. Further work could readily extend this approach from homodimers and oligomers to binary, ternary, and higher oligomer systems containing any number of different dyes or fluorescent proteins in precisely engineered arrangements.

■ AUTHOR INFORMATION

Corresponding Author

*E-mail: quentin.hanley@ntu.ac.uk.

Notes

The authors declare no competing financial interest.

■ ACKNOWLEDGMENTS

Z.G., Q.H., and L. B. acknowledge funding from NanoSci-E+ to the NanoActuate consortium. In the UK, NanoActuate is administered by EPSRC as EP/H00694X/1. In The Netherlands, NanoActuate is funded through STW grant 11022-NanoActuate. Also, we thank H. D. Nguyen and D. T. Dang for plasmid pHT581 and help with protein expression.

■ REFERENCES

(1) Bouvier, M. (2001) Oligomerization of G-protein-coupled transmitter receptors. *Nat. Rev. Neurosci. 2*, 274−286.

(2) Sacchettini, J. C., Baum, L. G., and Brewer, C. F. (2001) Multivalent protein−carbohydrate interactions. a new paradigm for supermolecular assembly and signal transduction. *Biochemistry 40*, 3009−3015.

(3) Li, S., Zhang, X., and Wang, W. (2010) Cluster formation of anchored proteins induced by membrane-mediated interaction. *Biophys. J. 98*, 2554−2563.

(4) Beckett, D. (2001) Regulated assembly of transcription factors and control of transcription initiation. *J. Mol. Biol. 314*, 335−352.

(5) Herrmann, H., Häner, M., Brettel, M., Ku, N.-O., and Aebi, U. (1999) Characterization of distinct early assembly units of different intermediate filament proteins. *J. Mol. Biol. 286*, 1403−1420.

(6) Pollard, T. D. (1986) Mechanism of actin filament self-assembly and regulation of the process by actin-binding proteins. *Biophys. J. 49*, 149−151.

(7) Zeugolis, D. I., Paul, R. G., and Attenburrow, G. (2008) Post-self-assembly experimentation on extruded collagen fibres for tissue engineering applications. *Acta Biomaterialia 4*, 1646−1656.

(8) Conrado, R. J., Wu, G. C., Boock, J. T., Xu, H., Chen, S. Y., Lebar, T., Turnšek, J., Tomšič, N., Avbelj, M., Gaber, R., Koprivnjak, T., Mori, J., Glavnik, V., Vovk, I., Benčina, M., Hodnik, V., Anderluh, G., Dueber, J. E., Jerala, R., and DeLisa, M. P. (2012) DNA-guided assembly of biosynthetic pathways promotes improved catalytic efficiency. *Nucleic Acids Res. 40*, 1879−1889.

(9) Le Gac, S., Schwartz, E., Koepf, M., Cornelissen, J. J. L. M., Rowan, A. E., and Nolte, R. J. M. (2010) Cysteine-containing polyisocyanides as versatile nanoplatforms for chromophoric and bioscaffolding. *Chem.—Eur. J. 16*, 6176−6186.

(10) Griffith, B. R., Allen, B. L., Rapraeger, A. C., and Kiessling, L. L. (2004) A polymer scaffold for protein oligomerization. *J. Am. Chem. Soc. 126*, 1608−1609.

(11) Delebecque, C. J., Lindner, A. B., Silver, P. A., and Aldaye, F. A. (2011) Organization of intracellular reactions with rationally designed RNA assemblies. *Science 333*, 470−474.

(12) Uhlenheuer, D. A., Milroy, L.-G., Neirynck, P., and Brunsveld, L. (2011) Strong supramolecular control over protein self-assembly using a polyamine decorated β-cyclodextrin as synthetic recognition element. *J. Mater. Chem. 21*, 18919−18922.

(13) Uhlenheuer, D. A., Wasserberg, D., Haase, C., Nguyen, H. D., Schenkel, J. H., Huskens, J., Ravoo, B. J., Jonkheijm, P., and Brunsveld, L. (2012) Directed supramolecular surface assembly of SNAP-tag fusion proteins. *Chem.—Eur. J. 18*, 6788−6794.

(14) Li, H., Park, S. H., Reif, J. H., LaBean, T. H., and Yan, H. (2003) DNA-templated self-assembly of protein and nanoparticle linear arrays. *J. Am. Chem. Soc. 126*, 418−419.

(15) Gangar, A., Fegan, A., Kumarapperuma, S. C., and Wagner, C. R. (2012) Programmable self-assembly of antibody−oligonucleotide conjugates as small molecule and protein carriers. *J. Am. Chem. Soc. 134*, 2895−2897.

(16) Sharma, R., Davies, A. G., and Wälti, C. (2012) Nanoscale programmable sequence-specific patterning of DNA scaffolds using RecA protein. *Nanotechnology 23*, 365301.

(17) Park, S. H., Yin, P., Liu, Y., Reif, J. H., LaBean, T. H., and Yan, H. (2005) Programmable DNA self-assemblies for nanoscale organization of ligands and proteins. *Nano Lett. 5*, 729−733.

(18) Diezmann, F., Eberhard, H., and Seitz, O. (2010) Native chemical ligation in the synthesis of internally modified oligonucleotide-peptide conjugates. *Pept. Sci. 94*, 397−404.

(19) Niemeyer, C. M. (2004) Semisynthetic DNA-protein conjugates for biosensing and nanofabrication. *Angew. Chem., Int. Ed. 49*, 1200−1216.

(20) Markwardt, M. L., Kremers, G. J., Kraft, C. A., Ray, K., Cranfill, P. J., Wilson, K. A., Day, R. N., Wachter, R. M., Davidson, M. W., and Rizzo, M. A. (2011) An improved cerulean fluorescent protein with enhanced brightness and reduced reversible photoswitching. *PloS One 6*, e17896.

(21) Reulen, S. W., van Baal, I., Raats, J. M., and Merkx, M. (2009) Efficient, chemoselective synthesis of immunomicelles using single-domain antibodies with a C-terminal thioester. *BMC Biotechnol. 9*, 66.

(22) Fu, J., Liu, M., Liu, Y., Woodbury, N. W., and Yan, H. (2012) Interenzyme substrate diffusion for an enzyme cascade organized on spatially addressable DNA nanostructures. *J. Am. Chem. Soc. 134*, 5516−5519.

(23) Erkelenz, M., Kuo, C.-H., and Niemeyer, C. M. (2011) DNA-mediated assembly of cytochrome P450 BM3 subdomains. *J. Am. Chem. Soc. 133*, 16111−16118.

(24) Hachikubo, Y., Iwai, S., and Uyeda, T. Q. P. (2010) Photoregulated assembly/disassembly of DNA-templated protein arrays using modified oligonucleotide carrying azobenzene side chains. *Biotechnol. Bioeng. 106*, 1−8.

(25) Chen, C.-h. B., Dellamaggiore, K. R., Ouellette, C. P., Sedano, C. D., Lizadjohry, M., Chernis, G. A., Gonzales, M., Baltasar, F. E., Fan, A. L., Myerowitz, R., and Neufeld, E. F. (2008) Aptamer-based

endocytosis of a lysosomal enzyme. *Proc. Natl. Acad. Sci. U.S.A. 105*, 15908−15913.
(26) Prencipe, G., Maiorana, S., Verderio, P., Colombo, M., Fermo, P., Caneva, E., Prosperi, D., and Licandro, E. (2009) Magnetic peptide nucleic acids for DNA targeting. *Chem. Commun. 40*, 6017−6019.
(27) Chakrabarti, R., and Klibanov, A. M. (2003) Nanocrystals modified with peptide nucleic acids (PNAs) for selective self-assembly and DNA detection. *J. Am. Chem. Soc. 125*, 12531−12540.
(28) de Koning, M. C., van der Marel, G. A., and Overhand, M. (2003) Synthetic developments towards PNA-peptide conjugates. *Curr. Opin. Chem. Biol. 7*, 734−740.
(29) Muir, T. W., Sondhi, D., and Cole, P. A. (1998) Expressed protein ligation: a general method for protein engineering. *Proc. Natl. Acad. Sci. U.S.A. 95*, 6705−6710.
(30) Hackenberger, C. P., and Schwarzer, D. (2008) Chemoselective ligation and modification strategies for peptides and proteins. *Angew. Chem., Int. Ed. 47*, 10030−10074.
(31) Duburcq, X., Olivier, C., Malingue, F., Desmet, R., Bouzidi, A., Zhou, F., Auriault, C., Gras-Masse, H., and Melnyk, O. (2004) Peptide-protein microarrays for the simultaneous detection of pathogen infections. *Bioconjugate Chem. 15*, 307−316.
(32) Lovrinovic, M., Seidel, R., Wacker, R., Schroeder, H., Seitz, O., Engelhard, M., Goody, R. S., and Niemeyer, C. M. (2003) Synthesis of protein-nucleic acid conjugates by expressed protein ligation. *Chem. Commun. 7*, 822−823.
(33) Hofmann, R. M., and Muir, T. W. (2002) Recent advances in the application of expressed protein ligation to protein engineering. *Curr. Opin. Biotechnol. 13*, 297−303.
(34) Nilsson, B. L., Soellner, M. B., and Raines, R. T. (2005) Chemical synthesis of proteins. *Annu. Rev. Biophys. Biomol. Struct. 34*, 91−118.
(35) Flavell, R. R., and Muir, T. W. (2009) Expressed protein ligation (EPL) in the study of signal transduction, ion conduction, and chromatin biology. *Acc. Chem. Res. 42*, 107−116.
(36) Menchise, V., De Simone, G., Tedeschi, T., Corradini, R., Sforza, S., Marchelli, R., Capasso, D., Saviano, M., and Pedone, C. (2003) Insights into peptide nucleic acid (PNA) structural features: the crystal structure of a D-lysine-based chiral PNA-DNA duplex. *Proc. Natl. Acad. Sci. U.S.A. 100*, 12021−12026.
(37) Nielsen, P. E. (2002) *Peptide Nucleic Acids: Methods and Protocols*, Humana Press Inc., USA.
(38) Drake, T. J., and Tan, W. (2004) Molecular beacon DNA probes and their bioanalytical applications. *Appl. Spectrosc. 58*, 269A−280A.
(39) Kuhn, H., Demidov, V. V., Gildea, B. D., Fiandaca, M. J., Coull, J. C., and Frank-Kamenetskii, M. D. (2001) PNA beacons for duplex DNA. *Antisense & Nucleic Acid Drug Development 11*, 265−270.
(40) Kuhn, H., Demidov, V. V., Coull, J. M., Fiandaca, M. J., Gildea, B. D., and Frank-Kamenetskii, M. D. (2002) Hybridization of DNA and PNA molecular beacons to single-stranded and double-stranded DNA targets. *J. Am. Chem. Soc. 124*, 1097−1103.
(41) Uhlenheuer, D. A., Wasserberg, D., Nguyen, H., Zhang, L., Blum, C., Subramaniam, V., and Brunsveld, L. (2009) Modulation of protein dimerization by a supramolecular host - guest system. *Chem.—Eur. J. 15*, 8779−8790.
(42) Zhou, Y., Dickenson, J. M., and Hanley, Q. S. (2009) Imaging lifetime and anisotropy spectra in the frequency domain. *J. Microsc. 234*, 80−88.
(43) Lakowicz, J. R. (2006) *Principles of Fluorescence Spectroscopy*, Springer, USA.
(44) Runnels, L. W., and Scarlata, S. F. (1995) Theory and application of fluorescence homotransfer to melittin oligomerization. *Biophys. J. 69*, 1569−1583.
(45) Gautier, I., Tramier, M., Durieux, C., Coppey, J., Pansu, R. B., Nicolas, J. C., Kemnitz, K., and Coppey-Moisan, M. (2001) Homo-FRET microscopy in living cells to measure monomer-dimer transition of GFP-tagged proteins. *Biophys. J. 80*, 3000−3008.
(46) Sun, Y., Wallrabe, H., Booker, C. F., Day, R. N., and Periasamy, A. (2010) Three-color spectral FRET microscopy localizes three interacting proteins in living cells. *Biophys. J. 99*, 1274−1283.
(47) Sun, Y., Wallrabe, H., Seo, S. A., and Periasamy, A. (2011) FRET microscopy in 2010: the legacy of Theodor Forster on the 100th anniversary of his birth. *ChemPhysChem 12*, 462−474.
(48) Sun, Y., Booker, C. F., Kumari, S., Day, R. N., Davidson, M., and Periasamy, A. (2009) Characterization of an orange acceptor fluorescent protein for sensitized spectral fluorescence resonance energy transfer microscopy using a white-light laser. *J. Biomed. Opt. 14*, 054009.
(49) Piston, D. W., and Kremers, G. J. (2007) Fluorescent protein FRET: the good, the bad and the ugly. *Trends Biochem. Sci. 32*, 407−414.
(50) Day, R. N., Booker, C. F., and Periasamy, A. (2008) Characterization of an improved donor fluorescent protein for Forster resonance energy transfer microscopy. *J. Biomed. Opt. 13*, 031203.
(51) Alvarado-González, M., Gallo, M., Lopez-Albarran, P., Flores-Holguín, N., and Glossman-Mitnik, D. (2012) DFT study of the interaction between the conjugated fluorescein and dabcyl system, using fluorescene quenching method. *J. Mol. Model. 18*, 4113−4120.
(52) Štefl, M., James, N. G., Ross, J. A., and Jameson, D. M. (2011) Applications of phasors to in vitro time-resolved fluorescence measurements. *Anal. Biochem. 410*, 62−69.
(53) Forde, T. S., and Hanley, Q. S. (2006) Spectrally resolved frequency domain analysis of multi-fluorophore systems undergoing energy transfer. *Appl. Spectrosc. 60*, 1442−1452.
(54) Subramaniam, V., Hanley, Q. S., Clayton, A. H., and Jovin, T. M. (2003) Photophysics of green and red fluorescent proteins: implications for quantitative microscopy. *Methods Enzymol. 360*, 178−201.
(55) Bader, A. N., Hofman, E. G., Voortman, J., van Bergen en Henegouwen, P. M. P., and Gerritsen, H. C. (2009) Homo-FRET imaging enables quantification of protein cluster sizes with subcellular resolution. *Biophys. J. 97*, 2613−2622.